Int. J. Electrochem. Sci., 11 **(2016)** 7527 – 7539, doi: 10.20964/2016.09.65

International Journal of ELECTROCHEMICAL SCIENCE
www.electrochemsci.org

A Novel Composite Obtained Through of Chemical Interaction of Zirconium (IV) Phosphated with Silver Hexacyanoferrate (III) for Voltammetric Detection of L-cysteine

Tayla Fernanda S. Da Silveira, Daniela S. Fernandes, Mariana de Souza Magossi, Priscila Fernanda P. Barbosa, Tamires R. Souza, Maiara de Souza Magossi, Devaney R. Do Carmo[*]

Faculdade de Engenharia de Ilha Solteira, Universidade Estadual Paulista "Júlio de Mesquita Filho", Departamento de Física e Química, Av. Brasil Centro, 56, Ilha Solteira-SP, Brasil. CEP. 15.385-000.
[*]E-mail: docarmo@dfq.feis.unesp.br

Received: 12 May 2016 / *Accepted:* 16 July 2016 / *Published:* 7 August 2016

A novel composite obtained from reaction of zirconium (IV) phosphated (ZrP) with Ag^{+} and subsequent interaction of potassium hexacyanoferrate (III) (ZrPAgH) was prepared and characterized by infrared spectroscopy (FTIR) and cyclic voltammetry. The graphite paste electrode modified with ZrPAgH exhibited a cyclic voltammogram with a redox couple with midpoint potential $E^{\theta'}$ = 0.70 V (*vs* $Ag/AgCl_{(sat.)}$), attributed to the Ag^{I}-CN-Fe^{II}/Ag^{I}-CN-Fe^{III} process (40% *w/w*; KNO_3 1.0 mol L^{-1}; *v* = 20 mV s^{-1}). The graphite paste electrode modified with ZrPAgH can be used in the electrocatalytic oxidation of L-cysteine in a linear range from 1.0×10^{-5} mol L^{-1} to 8.0×10^{-5} mol L^{-1} (*R* = 0.995) with detection limit of 1.02×10^{-5} mol L^{-1} and amperometric sensitivity of 2.40 mA/mol L^{-1}.

Keywords: Cyclic Voltammetry; Graphite Paste; L-cysteine; Silver Hexacyanoferrate (III); Zirconium Phosphated.

1. INTRODUCTION

Zirconium phosphated is a composite formed from Zr (IV) and phosphate groups. The chemistry of zirconium phosphated is of great interest due to its ion exchange, catalytic and ionic conduction properties. Moreover, it is a highly insoluble compound and has a good thermal stability [1,2]. The zirconium phosphated is typically obtained as an amorphous gelatinous precipitate when an excess of phosphoric acid or soluble phosphate is added to a zirconium salt soluble [1]. The phase obtained by refluxing of the amorphous gel in phosphoric acid normally is the zirconium bis (monohydrogen orthophosphate) monohydrate, $Zr(HPO_4)_2.H_2O$, conveniently called -zirconium

phosphated (-ZrP) [3]. The ZrP is considered the archetype of this class of compounds and its structure is formed from the packing of layers each of which consists of zirconium atoms, lying in a plane between O_3POH groups placed alternately above and below the metal atom plane [2].

The zirconium phosphated has been widely used in various applications such as drug delivery [4], catalysis [5,6], nanocomposites [7,8], nuclear waste management [9]. Furthermore, these compounds can have high surface areas in addition to providing the formation of new chemically stable materials, which makes them attractive in the preparation of chemically modified electrodes.

Graphite modified electrode containing electron mediator compounds on different supports, can be used as mediator for electro-oxidation of several compounds [10-14]. This electrode offers many advantages when compared with conventional electrodes, for example, mercury electrodes have high toxicity and rapid deterioration of the electrode response. On other hand, platinum and gold electrodes can have the formation of oxides on the surface, which could affect their analytical applications [15-17]. Furthermore, the graphite modified electrode is widely used due to the its low cost, convenient modification, versatility and low background current [18].

In this paper we report the study of the voltammetric behavior of a hybrid material obtained from the reaction between the zirconium phosphated (ZrP) and Ag^+ ions (ZrPAg), and its subsequent reaction with potassium hexacyanoferrate (III) (ZrPAgH). In this article, the new material, after the initial optimization conditions, was tested in the electrocatalytic oxidation of L-cysteine.

L-cysteine (L-2-amino-3-mercaptopropionic acid) is a biologically important amino acid which contains sulfur and is involved in a variety of important cellular functions. The cysteine biological reactions are accompanied by an exchange reaction of SH/SS, and the conversion of the disulfide in a dithiol group [19,20]. Many methods have been developed for the determination of L-cysteine, including HPLC [21], spectrophotometry [22], capillary electrophoresis [23]. However, most methods have some disadvantages such as low sensitivity, high costs, complexity, processing the sample, among others, which prevents their practical application [24,25]. Thus, electrochemical methods have been the most favorable methods for the determination of thiols (especially L-cysteine) for presenting inherent advantages of simplicity, rapidity and high sensitivity [25,26]. However, high overpotentials of electrochemical oxidation are required for thiols at the conventional electrodes [25,27]. In order to overcome these problems, many strategies have been employed. Among them stands out the use of chemically modified electrodes [28-31].

2. EXPERIMENTAL

2.1 Reagents and solutions

All solvents and reagents were of analytical purity (Merck or Aldrich) and were utilized as purchased and L-cysteine was used without further purification. All solutions and supporting electrolytes were prepared using Milli-Q water. The L-cysteine solution was prepared immediately before the voltammetric analysis.

2.2 Synthesis of Zirconium Phosphated (ZrP)

The synthesis of the zirconium phosphated was carried out as follows: 4 g of zirconium (IV) isopropoxide isopropanol complex (Sigma-Aldrich) were added in 800 mL of deionized water, which were kept under stirring for 4 hours at 60 °C. Subsequently was added 400 mL of phosphoric acid solution 0.1 N and kept under stirring for 2 hours at 40 °C. The suspension was allowed to rest protected from light, for 30 hours. Then the solid phase was separated in a sintered funnel and washed with deionized water. The material was dried at 100 °C and described as ZrP.

2.3 Formation of complex ZrPAgH

Mixed valence complex was synthesized by adding of 1.0 g of ZrP in 25 mL of a solution of silver nitrate 1.0×10^{-3} mol L^{-1}. The mixture was stirred for 1h at room temperature. The solid phase was filtered, washed with deionized water and designated as ZrPAg. About 0.5 g of ZrPAg was added to a solution of 1.0×10^{-3} mol L^{-1} of potassium hexacyanoferrate (III) and the mixture was stirred for 1 hour and then the solid filtered, washed with deionized water and dried at room temperature. The material resulting was described by ZrPAgH [12].

2.4 Preparation of the graphite paste electrode modified with ZrPAgH

The graphite paste electrode modified with ZrPAgH was prepared by mixing 40 mg of ZrPAgH with 60 mg of graphite and 20 μL of mineral oil. The electrode body was produced from a glass tube of 3 mm i.d. and 14 cm height, containing graphite paste. A copper wire was inserted through the opposite end of the glass tube to establish electrical contact [10, 13 29].

2.5 Techniques

2.5.1 Fourier transform infrared spectra

Fourier transform infrared spectra were recorded on a Nicolet 5DXB FT-IR 300 spectrometer. Approximately 600 mg of KBr was ground in a mortar/pestle, and sufficient solid sample was ground with KBr to produce a 1 wt.% mixture resulting in KBr pellets. After the sample was loaded, the sample chamber was purged with nitrogen for a minimum of 10 min prior to data collection. A minimum of 32 scans was collected for each sample at a resolution of 4 cm^{-1} [29].

2.5.2 Electrochemical Measurements

The electrochemical measurements were performed using an electrochemical system with a AUTOLAB PGSTAT (Metrohm Pensalab) potentiostat. It was used a modified working electrode (graphite paste electrode), a reference electrode ($Ag/AgCl_{(sat)}$) and a platinum wire as the auxiliary electrode. The modified graphite paste was prepared by mixing graphite/modifier (ZrPAgH) in different proportions (10, 20, 30, 40 and 50% (*w/w*)) and 20 μL of mineral oil (Nujol) [10, 29]. It was

performed a preliminary study to select the best ratio of graphite paste. The measurements were carried out at 25 ºC. It were carried out studies on different supporting electrolytes, such as KNO_3, $NaNO_3$, NH_4NO_3 and KCl.

2.5.3 Procedure

Cyclic voltammograms were recorded for study the sensibility of L-cysteine by graphite paste electrode modified with ZrPAgH. The supra analite solutions were prepared immediately before use. In most of the experiments, 1.0 mol L^{-1} KCl was used as the supporting electrolyte. The catalytic and sensibility current was estimated by the difference between the electrode current in the presence of analite compounds and that which is established in the blank solution [13].

3. RESULTS AND DISCUSSION

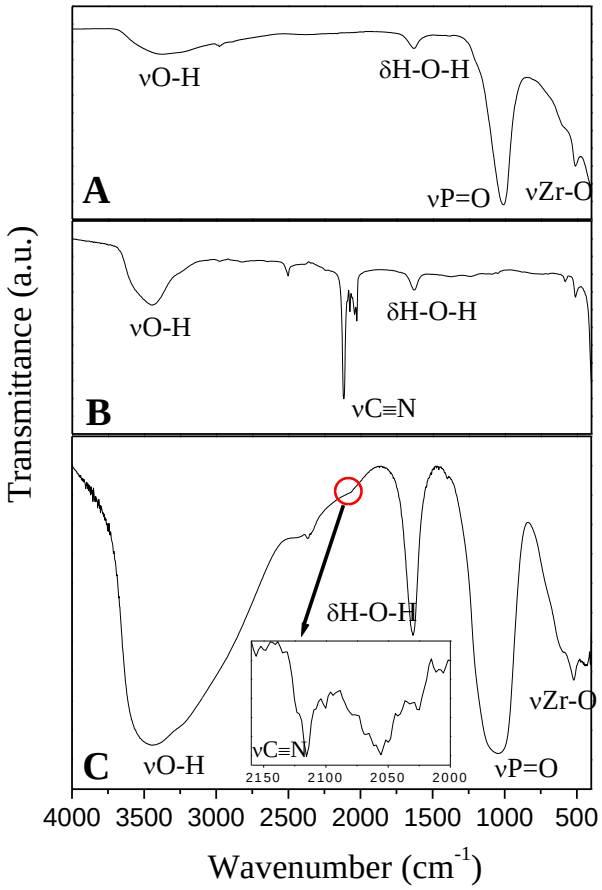

Figure 1. Vibrational spectra in the infrared region: (A) ZrP, (B) HCF and (C) ZrPAgH.

Figure 1 illustrates the vibrational spectra of the ZrP, potassium hexacyanoferrate (III) (HCF) and ZrPAgH. The spectrum exhibited by potassium hexacyanoferrate (III) (Fig. 1B) shows significant vibrations at ~2115 and 2035 cm^{-1}, which are related to the vibrations of the $C{\equiv}N_{(\nu C{\equiv}N)}$ bonding [13,

32,33]. For the spectrum of the ZrP illustrated in Figure 1A, a broad band between 3700 to 3000 cm^{-1} corresponding to the axial deformation of the $OH_{(\nu OH)}$ groups from adsorbed water molecules was observed in addition to a band at 1632 cm^{-1} attributed to the angular deformation $HOH_{(\delta HOH)}$. The absorption at ~1010 cm^{-1} was attributed to the $P{=}O_{(\nu P=O)}$ stretching [33,34]. Absorptions were also observed in the region between 580 to 400 cm^{-1} and correspond to the Zr-O bonds [35]. All the absorptions related to the spectrum of the ZrP it were also observed for spectrum of the ZrPAgH (Fig. 1C). Furthermore, the spectra exhibited vibrations at ~2115 and 2055 cm^{-1} related to the estiramento $C{\equiv}N_{(\nu C\equiv N)}$ stretching that is characteristic of the potassium hexacyanoferrate (III) precursor [13].

ZrPAgH was also characterized using cyclic voltammetry technique in order to investigate the presence of the metal complex formed as illustrated in Figure 2. Cyclic voltammogram of ZrPAgH exhibited one redox pair with $E^{\theta'}$ = 0.70 V, attributed to the Ag^{I}-CN-Fe^{II}/ Ag^{I}-CN-Fe^{III} process.

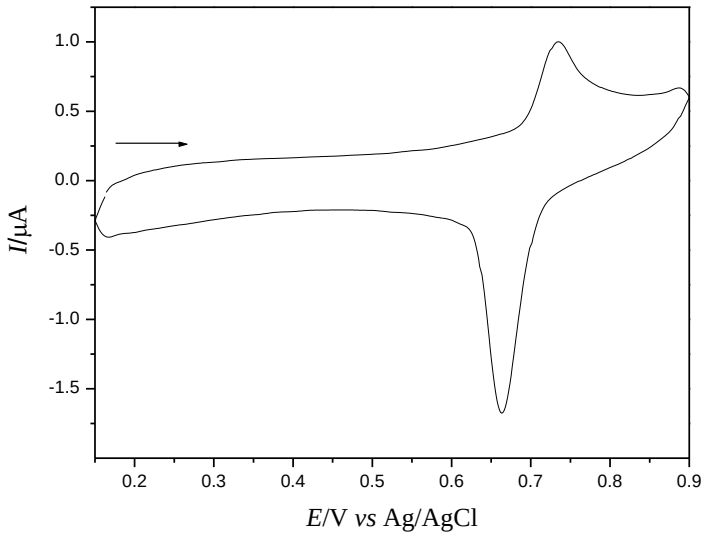

Figure 2. Cyclic voltammogram of graphite paste modified with ZrPAgH (40% *w/w*; v = 20 mV s^{-1}; KNO_3; 1.00 mol L^{-1}).

Figure 3 illustrates the studies carried out on different supporting electrolytes. It was observed that the nature of the cations affected the midpoint potential ($E^{\theta'}$) and the current intensities.

Additionally, it was observed that all of the cyclic voltammograms of ZrPAgH in presence of electrolyte of alkali metal nitrate showed one well-defined redox pair. However the best performance was observed for cyclic voltammogram obtained in the presence of KNO_3. This fact can be explained because the K^+ ion has a smaller hydration radius than Na^+ ion and a higher mobility compared to NH_4^+ ion [36]. On the other hand, the redox process is inhibited in presence of KCl as supporting electrolyte, due to the formation of $AgCl_{(sat.)}$ on the electrode surface. In addition, when employing KCl, a new redox process with $E^{\theta'}$=0.35 V is present and must be related to the electroactive nature of ZrP, which is active when Ag^{I}-CN-Fe^{II}/ Ag^{I}-CN-Fe^{III} process is inhibited.

Table 1 lists the main electrochemical parameters obtained from the cyclic voltammetry of graphite paste modified with ZrPAgH in different electrolytes.

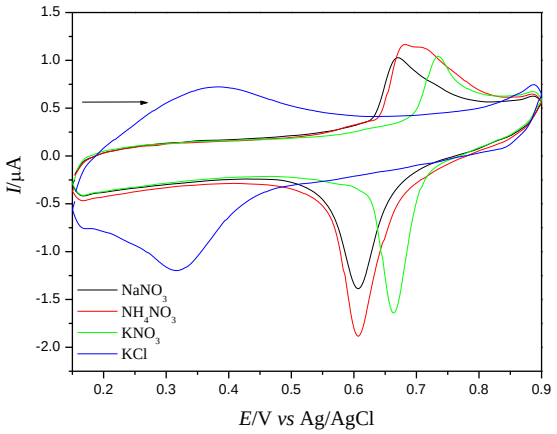

Figure 3. Cyclic voltammograms of graphite electrode modified with ZrPAgH in differents supporting electrolytes: KNO_3, $NaNO_3$, NH_4NO_3 and KCl (40% *w/w*, *v* = 20 mV s^{-1}, 1.00 mol L^{-1}).

Table 1. Electrochemical parameters of the graphite paste modified with ZrPAgH in different supporting electrolytes (40% *w/w*, *v* = 20 mV s^{-1}, 1.00 mol L^{-1}).

Supporting electrolyte	*Ipa* (µA)	*Ipc* (µA)	|*Ipa/Ipc*|	*Epa* (V)	*Epc* (V)	Δ*Ep* (V)	$E^{\theta'}$ (V)	Diameter of the hydrated cation (nm)*
KNO_3	0.79	-1.34	0.59	0.73	0.66	0.70	0.07	0.24
$NaNO_3$	0.73	-1.03	0.71	0.67	0.61	0.64	0.06	0.36
NH_4NO_3	0.87	-1.34	0.65	0.69	0.61	0.65	0.08	0.24
KCl	0.49	-0.66	0.74	0.38	0.32	0.35	0.06	0.24

*[37,38]

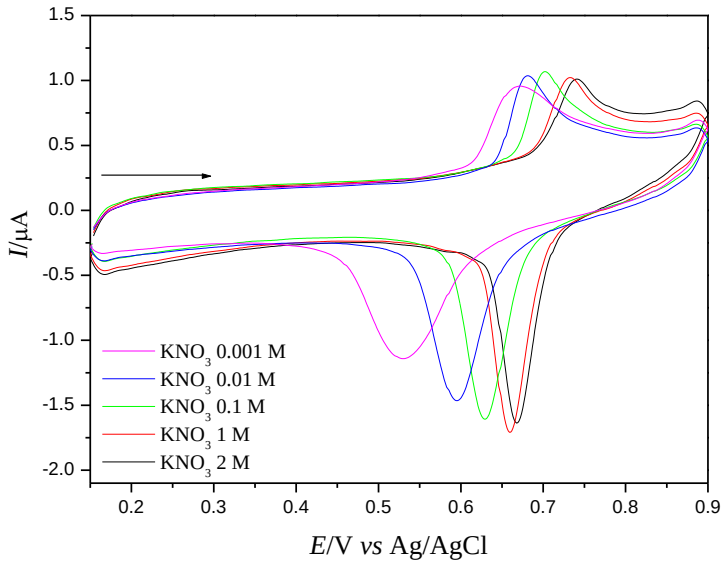

Figure 4. Cyclic voltammograms of graphite electrode modified with ZrPAgH in differents supporting electrolyte concentrations (40% *w/w*, *v* = 20 mV s^{-1}).

Figure 4 illustrates the cyclic voltammograms of graphite paste modified with ZrPAgH in different concentrations of KNO_3 (0.001 mol L^{-1} to 2.0 mol L^{-1}). It was observed that the performance becomes different and there is an increase in the current intensity with increasing concentration of supporting electrolyte [39]. Furthermore, there was a displacement of midpoint potential $E^{\theta'}$ for positive values (0.60 to 0.71 V) with increasing concentration, indicating the involvement of K^+ ions in the redox process [28]. The increasing concentration of supporting electrolyte makes difficult the start of the oxidation process, however, it is notable that the redox process occurs faster and more well defined at the highest concentrations.

It was found a linear relationship between the midpoint potential and the logarithm (log) of the K^+ ions concentration, as illustrated by Figure 5. It suggests that the redox process is highly dependent on the concentration of K^+ [39]. The line slope was of 32.5 mV per decade of potassium ions, indicating that the behavior exhibited by the electrode approaches a nerstian process [39, 40] with transfer of two electrons.

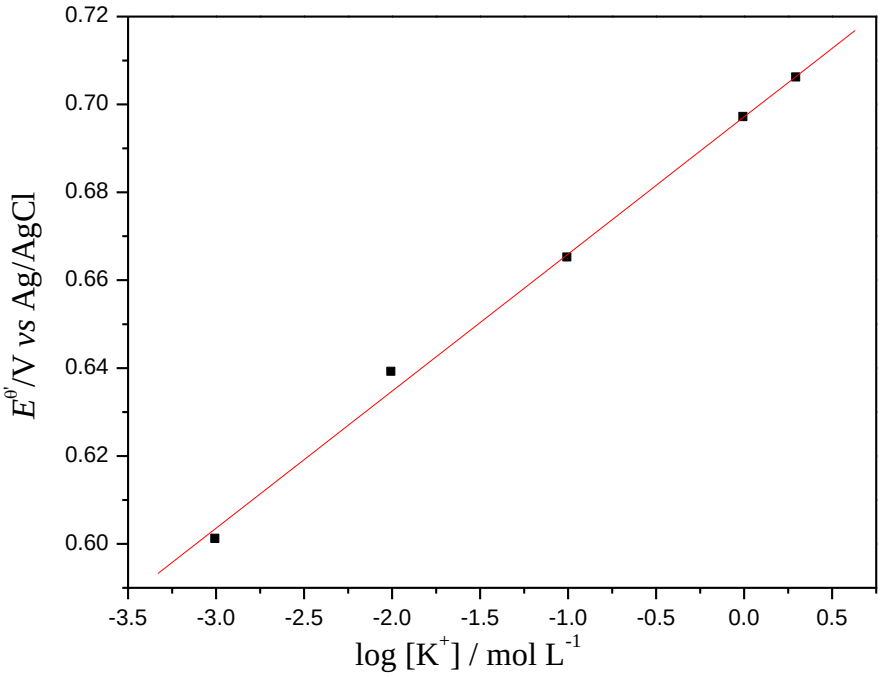

Figure 5. Midpoint potential ($E^{\theta'}$) of graphite paste modified with ZrPAgH as a function of KNO_3 concentration.

After this study, the concentration of the supporting electrolyte chosen to continue the ensuing studies was 1.00 mol L^{-1} due to the better voltammetric performance.

A study with different hydrogen ion concentrations (pH 1.00 to 8.00) was performed for the ZrPAgH. Cyclic voltammograms illustrated in Figure 6 showed that the anodic current intensity varied between 0.94 and 0.89 μA and $E^{\theta'}$ remained constant about 0.70 V. In this case it can be verified that the hydrogen ion concentration hardly affects the electrochemical process.

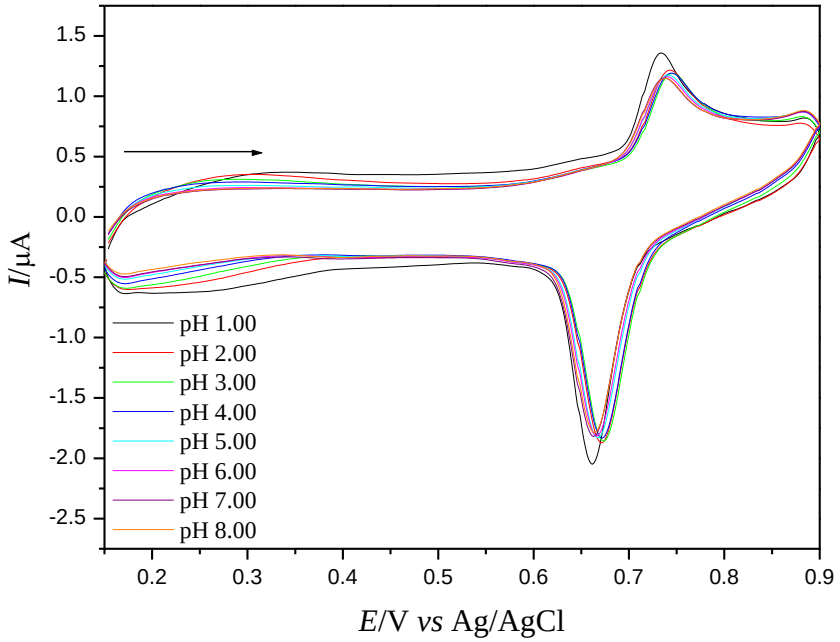

Figure 6. Cyclic voltammograms of the graphite paste modified with ZrPAgH at different pH values (1.0 to 8.0); (40% *w/w*, v = 20 mV s^{-1}, KCl 1.00 mol L^{-1}).

The pH value chosen for further studies was pH 7.00, since there is the possibility of conducting studies to determination electrocatalytic of drugs in a biological environment [13, 39].

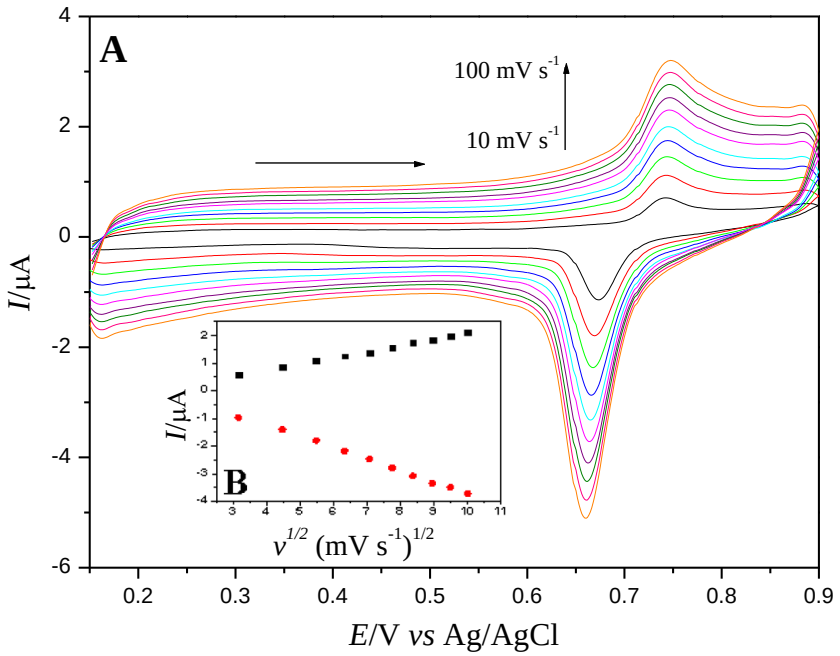

Figure 7. (A) Cyclic voltammograms of the graphite paste modified with ZrPAgH at different scan rates (10-100 mV s^{-1}) (40% *w/w*, KNO_3 1.00 mol L^{-1}, pH 7.00). (B) Dependence on current intensity of the anodic and cathodic peaks with the square root of the scan rate.

Figure 7 (A) illustrates the cyclic voltammograms of ZrPAgH at different scan rates (10-100 mV s^{-1}). It was observed that by increasing the scan rate there is an increase in the current intensity and $E^{\theta'}$ remained constant about 0.71 V. It was observed that the scan rate increase provides an increase in the resistance, causing an increase in ΔEp at higher scan rates [39]. Figure 7 (B) illustrates the linear dependence of the current intensity of the anodic/cathodic peak and the square root of scan rate characterizes a diffusion process [10, 39, 41].

Table 2 lists the main electrochemical parameters obtained from the cyclic voltammetry of graphite paste modified with ZrPAgH at different scan rates.

Table 2. Electrochemical parameters of the graphite paste modified with ZrPAgH at different scan rates (40% *w/w*, KNO_3 1.00 mol L^{-1}, pH 7.00).

Scan rates (mV s^{-1})	Ipa (μA)	Ipc (μA)	|Ipa/Ipc|	Epa (V)	Epc (V)	$E^{\theta'}$ (V)	ΔEp (V)
10	0.57	-0.96	0.59	0.74	0.67	0.71	0.07
20	0.86	-1.40	0.61	0.74	0.67	0.71	0.07
30	1.08	-1.79	0.60	0.74	0.67	0.71	0.07
40	1.26	-2.18	0.58	0.74	0.67	0.71	0.07
50	1.39	-2.47	0.56	0.74	0.67	0.71	0.07
60	1.58	-2.78	0.57	0.75	0.66	0.71	0.09
70	1.77	-3.08	0.57	0.75	0.66	0.71	0.09
80	1.84	-3.35	0.55	0.75	0.66	0.71	0.09
90	1.99	-3.50	0.57	0.75	0.66	0.71	0.09
100	2.14	-3.72	0.58	0.75	0.66	0.71	0.09

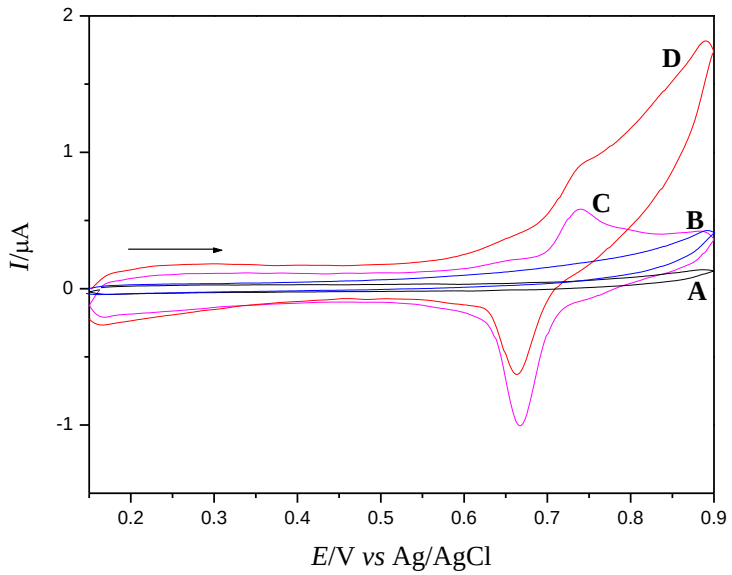

Figure 8. Cyclic voltammograms of: **(A)** graphite paste electrode unmodified in the absence of L-cysteine, (B) graphite paste electrode unmodified in presence of 8.00×10^{-5} mol L^{-1} of L-cysteine, (C) graphite paste electrode modified with ZrPAgH in the absence of L-cysteine and (D) graphite paste modified with ZrPAgH in presence of 8.00×10^{-5} mol L^{-1} of L-cysteine.

Figure 8 illustrates the electrocatalytic oxidation of L-cysteine in the graphite paste electrode modified with ZrPAgH. The curves A and B represent the graphite paste electrode unmodified in the absence and presence of L-cysteine (8.00×10^{-5} mol L^{-1}), respectively, and it was observed that both voltammograms showed no electroactivity in the potential range (0.15 and 0.90 V). The graphite paste electrode modified with ZrPAgH (C) exhibited a redox couple with $E^{\theta'}$=0.70 V in the absence of L-cysteine and showed an increase in the anodic peak current intensity followed by a decrease in the intensity in the cathodic peak current intensity in the presence of L-cysteine (D).

The equation for the electrochemical oxidation of L-cysteine, as described in the literature [28, 42] can be represented as follows:

$$2\ \text{L-cysteine (CySH)} \rightleftharpoons \text{L-cystine (CySSCy)} + 2H^+ + 2e^- \qquad \text{(Eq. 1)}$$

The anodic peak current intensity increases due to the electrocatalytic oxidation of L-cysteine. The Fe (III) produced during the anodic scan chemically oxidizes L-cysteine, whereas Fe (III) is reduced to Fe (II), which will again be electrochemically oxidized to Fe (III) [39, 10]. The electrochemical and chemical stages of the system are represented by equations 2 and 3, respectively.

EE $$2\ KAg_3[Fe^{II}(CN)_6] \rightleftharpoons 2\ Ag_3[Fe^{III}(CN)_6] + 2K^+ + 2e^- \qquad \text{(Eq. 2)}$$

EC $$2\ Ag_3[Fe^{III}(CN)_6] + 2X + 2K^+ \rightleftharpoons 2\ KAg_3[Fe^{II}(CN)_6] + Y + 2H^+ \qquad \text{(Eq. 3)}$$

Where X = L-cysteine (CySH) ; Y = L-cystine (CySSCy).

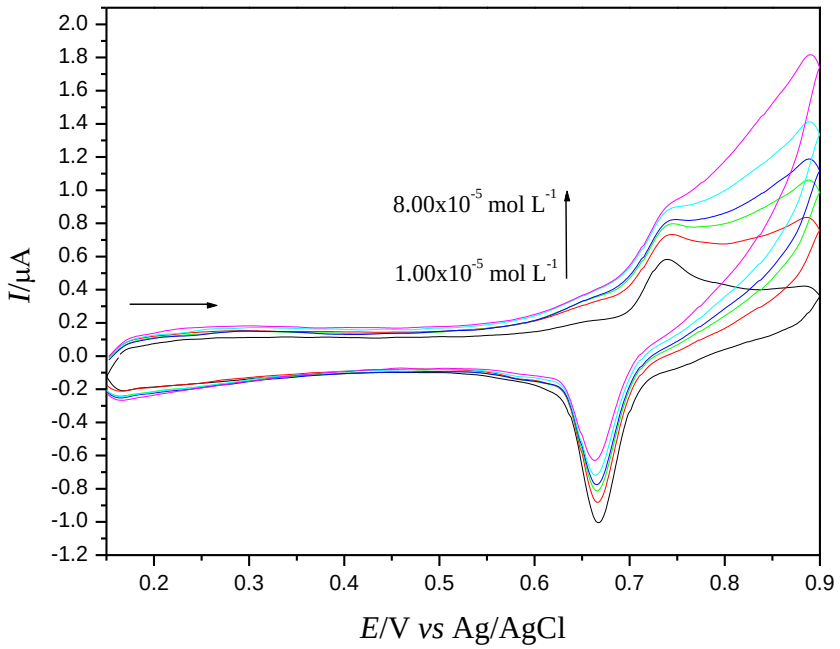

Figure 9. Cyclic voltammograms obtained for the graphite paste electrode modified with ZrPAgH in the presence of different L-cysteine concentrations (1.00×10^{-5} to 8.00×10^{-5} mol L^{-1}); (40% *w/w*, *v* = 20 mV s^{-1}, KNO_3, 1.00 mol L^{-1}, pH 7.00).

Figure 9 shows the voltammetric behavior of ZrPAgH after the additions of different aliquots of L-cysteine. The analytic curve, showing the anodic current as a function of L-cysteine concentration for ZrPAgH is illustrated in Figure 10. The modified graphite paste electrode showed a linear response in the concentration range of 1.00×10^{-5} to 8.00×10^{-5} mol L^{-1}, presented a corresponding equation Y (μA) = 0.57 + 2.59×10^{3} [L-cysteine] and a correlation coefficient R = 0.995. The detection limit obtained for this system was of 1.02×10^{-5} mol L^{-1} with a relative standard deviation of ± 3% (n = 3) and an amperometric sensitivity of 2.59 mA/mol L^{-1}.

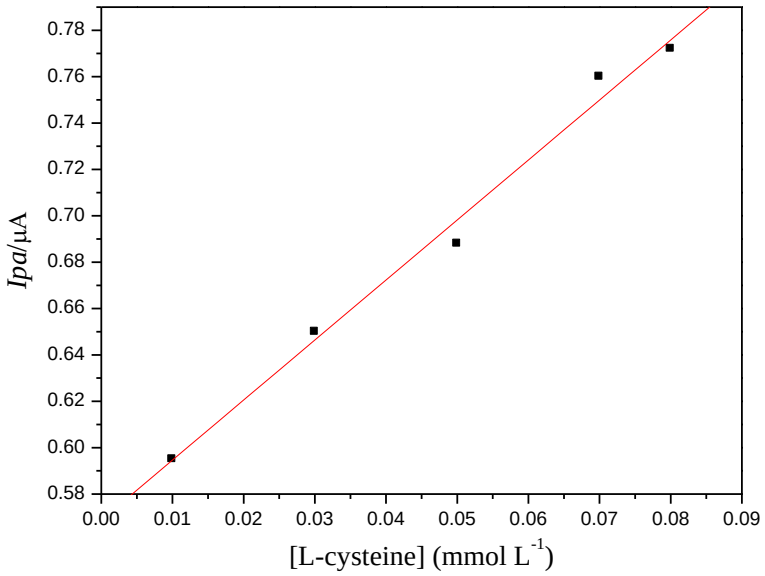

Figure 10. Analytic curve of the anodic peak current as a function of L-cysteine concentration using the graphite paste electrode modified with ZrPAgH (40% *w/w*, v = 20 mV s^{-1}, KNO_3, 1.00 mol L^{-1}, pH 7.00).

Table 3. Comparison of this work with previous reports of cysteine detection.

Electrode Material	Technique	Linear Range (M)	Limit Detection (M)	Reference
Oxovanadium(IV) Salen / GPE[(a)]	Chronoamperometry	2.40×10^{-4} to 2.30×10^{-3}	1.70×10^{-4}	[43]
PDMA / FMGPE[(b)]	Chronoamperometry	8.00×10^{-5} to 2.25×10^{-3}	6.17×10^{-5}	[44]
ErHCF / CCEs[(c)]	Chronoamperometry	5.00×10^{-6} to 1.30×10^{-4}	2.00×10^{-6}	[45]
MnHCF / GPE[(a)]	Cyclic Voltammetry	2.00×10^{-5} to 1.00×10^{-2}	4.80×10^{-6}	[46]
ZrPAgH / GPE[(a)]	Cyclic Voltammetry	1.00×10^{-5} to 8.00×10^{-3}	1.02×10^{-5}	This work

a = graphite paste electrode; *b* = film modified graphite paste electrode; *c* = carbon ceramic electrodes.

Table 3 presents a comparison of similar reports in the literature for L-cysteine detection. These results show the analytical benefits obtained by the use of ZrPAgH, which showed a good limit of detection when compared with previous reports.

4. CONCLUSION

A composite formed by interaction of Zr (IV) isopropoxide and phosphoric acid, followed by silver adsorption and subsequent reaction of hexacyanoferrate (III) (ZrPAgH), was incorporated into a graphite paste electrode and the electrochemical studies were conducted using the cyclic voltammetry technique. The cyclic voltammetric behavior of ZrPAgH presented a redox couple well defined with $E^{\theta'}$ = 0.70 V, assigned to Ag^{I}-CN-Fe^{II}/Ag^{I}-CN-Fe^{III} process (40% *w/w*; KNO_3 1.0 mol L^{-1}; ν = 20 mV s^{-1}). The graphite paste electrode modified with ZrPAgH allowed the electrocatalytic determination of L-cysteine. The modified electrode gives a linear response in the concentration range of 1.00×10^{-5} to 8.00×10^{-5} mol L^{-1}, presented a corresponding equation Y (μA) = 0.57 + 2.59×10^{3} [L-cysteine] and a correlation coefficient R = 0.995. The detection limit obtained for this system was of 1.02×10^{-5} mol L^{-1} with a relative standard deviation of ± 3% (n = 3) and amperometric sensitivity of 2.59 mA/mol L^{-1} for L-cysteine. Thus, the novel composite (ZrPAgH) is a potential candidate for the construction of electrochemical sensors for the determination of L-cysteine.

ACKNOWLEDGEMENTS
The authors are grateful for Fundação de Amparo à Pesquisa do Estado de São Paulo (FAPESP - Proc. 2013/08495-9; 2012/05438-1 and 2012/11306-0).

References

1. A. Clearfield, J.A. Stynes, *J. Inorg. Nucl. Chem*., 26(1) (1964) 117-129.
2. U. Costantino, F. Marmottini, M. Curini, O. Rosati, *Catal. Lett.*, 22 (1993) 333-336.
3. A. Clearfield, W.L. Duax, A.S. Medina, G.D. Smith, J.R. Thomas, *J. Phys. Chem*., 73(10) (1969) 3424-3430.
4. V. Saxena, A. Diaz, A. Clearfield, J.D. Batteasb, M.D. Hussain, *Nanoscale*, 5(6) (2013) 2328-2336.
5. I.A. Stenina, A.B. Il'in, S.D. Kirik, N.A. Zhilyaeva, G.Yu. Yurkovd, A.B. Yaroslavtsev, *Inorg. Mater*., 50(6) (2014) 586-591.
6. Y. Zhou, R. Huang, F. Ding, A.D. Brittain, J. Liu, M. Zhang, M. Xiao, Y. Meng, L. Sun, *ACS Appl. Mater. Inter*., 6(10) (2014) 7417-7425.
7. H. Wu, C. Liu, J. Chen, Y. Yanga, Y. Chen, *Polym. Int*., 59(7) (2010) 923-930.
8. *B.M. Mosby, A. Díaz, V. Bakhmutov, A. Clearfield,* ACS Appl. Mater. Inter., *6(1) (2014) 585-592.*
9. B.E. Scheetz, D.K. Agrawal, E. Breval, R. Roy, *Waste Manage*, 14(6) (1994) 489-505.
10. L.A. Soares, W. Yingzi, T.F.S. Da Silveira, D.R. Silvestrini, U.O. Bicalho, N.L. Dias Filho, D.R. Do Carmo, *Int. J. Electrochem. Sci.,* 8 (2013) 7565–7580.
11. L.A. Soares, T.F.S. Da Silveira, D.R. Silvestrini, U.O. Bicalho, N.L. Dias Filho, D.R. Do Carmo, *Int. J. Electrochem. Sci.,* 8 (2013) 4654–4669.
12. L.R. Cumba, U.O. Bicalho, D.R. Silvestrini, D.R. Do Carmo, *Int. J. Chem*., 4(2) (2012) 66-78.
13. T.F.S. Da Silveira, D.R. Silvestrini, U.O. Bicalho, D.R. Do Carmo, *Int. J. Electrochem. Sci*., 8 (2013) 872–886.
14. A.R.F. Pipi, D.R. Do Carmo, *J. Appl. Electrochem.*, 41 (2011) 787-793.
15. R.F. Bergstron, D.R. Kay, J.G. Wagner, *J. Chromatogr. B Biomed. Sci. Appl*., 222(3) (1981) 445-452.
16. D.R. Do Carmo, R.M. Da Silva, N.R. Stradiotto, *J. Braz. Chem. Soc*., 14(4) (2003) 616-620.
17. M.E. Johll, D.G. Williams, D.C. Johnson, *Electroanal*., 9(18) (1997) 1397-1402.

18. A.C. Pereira, A.S. Santos, L.T. Kubota, *Quim. Nova*, 25(6) (2002) 1012-1021.
19. L.H. Wang, W.S. Huang, *Sensors*, 12(3) (2012) 3562-3577.
20. M. Ahmad, C. Pan, J. Zhu, *J. Mater. Chem.*, 20 (2010) 7169-7174.
21. A.M. Di Pietra, R. Gotti, D. Bonazzi, V. Andrisano, V. Cavrini, *J. Pharm. Biom. Anal*., 12(1) (1994) 91-98.
22. M.S. Garcia, C. Sanchez-Pedreno, I. Albero, *Analyst*, 115(7) (1990) 989–992.
23. Y. Tao, X. Zhang, J. Wang, X. Wang, N. Yang, *J. Electroanal. Chem*., 674 (2012) 65-70.
24. X. Liu, H. Lv, Q. Sun, Y. Zhong, J. Zhao, J. Fu, M. Lin, J. Wang, *Anal. Lett*., 45(15) (2012) 2246-2256.
25. C. Xiao, J. Chen, B. Liu, X. Chu, L. Wu, S. Yao, *Phys. Chem. Chem. Phys.*, 13(4) (2010) 1568-1574.
26. M. Ahmad, C. Pan, J. Zhu, *J. Mater. Chem.*, 20(34) (2010) 7169-7174.
27. M. Song-Jiang, L. Sheng-Lian, Z. Hai-Hui, K. Ya-Fei, N. Xiao-Hui, *J. Cent. South. Univ. T.*, 15 (2008) 170-175.
28. L.R. Cumba, U.O. Bicalho, D.R. Do Carmo, *Int. J. Electrochem. Sci*., 7 (2012) 4465–4478.
29. D.R. Do Carmo, D.R. Silvestrini, T.F.S. Da Silveira, L.R. Cumba, N.L. Dias Filho, L.A. Soares, *Mater. Sci. Eng. C*, 57(1) (2015) 24-30.
30. S. Fei, J. Chen, S. Yao, G. Deng, D. He, Y. Kuang, *Anal. Biochem*., 339 (2005) 29-35.
31. C. Deng, J. Chen, X. Chen, M. Wang, Z. Nie, S. Yao, *Electrochim. Acta*, 54 (2009) 3298-3302.
32. D.L. Pavia, G.M. Lampman, G.S. Kriz, J.R. Vyvyan, *Introdução à espectroscopia*, Cengage Learning, São Paulo (2012).
33. R.M. Silverstein, F.X. Webster, D.J. Kiemle, *Spectrometric identification of organic compounds*, John Wiley & Sons, New York (2005).
34. R. Thakkar, U. Chudasama, *Electrochim. Acta*, 54 (2009) 2720-2726.
35. M. Pal, R.N. Kapoor, *Inorg. Chim. Acta*, 40 (1980) 99-103.
36. D. Jayasri, S.S. Narayanan, *Sens. Actuators B.*, 119(1) (2006) 135-142.
37. A. Abbaspour, A. Ghaffarinejad, *Electrochim. Acta*, 53(22) (2008) 6643-6650.
38. D. Engel, E.W. Grabner, *Berichte der Bunsengesellschaft fur Physikalische Chemie*, 89(9) (1985) 982-986.
39. D.R. Silvestrini, T.F.S Da Silveira, U.O. Bicalho, D.R. Do Carmo, *Int. J. Electrochem. Sci*., 10 (2015) 2839–2858.
40. D.R. Carmo, R.M. Silva, N.R. Stradiotto, *Eclet. Quim*., 27 (2002) 197-210.
41. A.J. Bard, L.R. Faulkner, *Electrochemical methods: fundamentals and Applications*. Wiley, New York (1980).
42. M. Zhou, J. Ding, L. Guo, Q. Shang, *Anal. Chem.*, 79(14) (2007) 5328-5335.
43. M.F.S. Teixeira, E.R. Dockal, E.T.G. Cavalheiro, *Sens. Actuators B*, 106(2) (2005) 619-625.
44. R. Ojani, J.B. Raoof, E. Zarei, *J. Electroanal. Chem.*, 638 (2010) 241-245.
45. Q.-L. Sheng, H. Yu, J.-B. Zheng, *J. Solid State Electrochem.*, 12 (2008) 1077-1084.
46. P. Wang, X. Jing, W. Zhang, G. Zhu, *J. Solid State Electrochem.*, 5 (2001) 369-374.